Effect of Geometric Design on Airflow Simulation Inside the Storage Room for Paddy

IOP Conf. Series: Materials Science and Engineering **501** (2019) 012040 doi:10.1088/1757-899X/501/1/012040

Effect of Geometric Design on Airflow Simulation Inside the Storage Room for Paddy

S Echaroj[1, *], N Pannucharoenwong[1] , P Vengsungnle[2], and M Wichangarm[3]

[1] Department of Mechanical Engineering, Faculty of Engineering, Thammasat University, 12120 Thailand.

[2] Department of Agricultural Machinery Engineering, Faculty of Engineering and Architecture, Rajamangala University of Technology Isan, 30000 Thailand.

[3] Department of Mechanical Engineering, Ubon Ratchathani University, 34190 Thailand

*Corresponding Author: snunkha@engr.tu.ac.th

Abstract. Stability of rice paddy organic content is essential for the production of high quality rice. For this reason it is important to design a proper storage room with sufficient ventilation and moisture removal capability. Airflow dynamics in terms of velocity profile were modelled through computational fluid dynamic (CFD) simulations in Fluent 6.3 program across the three different geometrical design of paddy storage room. The selection of turbulence model used in CFD is an important process due to the uncertainty of turbulence model in different operating scale. This research used a turbulence model and RNG k-ε model to calculate along the simulation of Discrete Ordinances (DO) type radiation and the heat flux was set to 800 W/m^2. The results of this study have shown that Model C with pyramid-like roof demonstrated the optimum moisture removal through convection mechanism with the lowest average velocity of 0.175 m/s and the average temperature of 365.88 K. The CFD technique could be suitable for the simulation of airflow, permitting decrease in time and cost in the evaluation of airflow inside storage facility for paddy rice.

1. Introduction

Rice or Oryza sativa L. is the principal food in most tropical continent including East, South, Southeast Asia and Latin America [1]. Countries including china, Japan, India, Pakistan, Vietnam and Thailand were found to supply 90% of rice consumed worldwide [2]. Due to significant economic expansion and population growth, the efficiency of rice production must incline by approximately 1% per year in order to guarantee sufficient food for everyone [3]. Thailand is the second largest exporter of rice with over 9.8 million tons in volume [4]. One of the main concern in rice production is during the storage period after cultivation of paddy rice. In Thailand, the moisture content of paddy rice immediately after harvest is 18 to 27% (wet basis), which is relatively high and likely to increase in conventional storage causing the quality of rice to decrease. The target moisture content of rice sold at mills need to be at least 14% (wet basis). In order to preserve the quality of paddy rice, the paddy content must be stabilized by appropriate storage construction. Inappropriate aeration system may resulted in problems associated with an increase in moisture content, insect and spoilage [5].

Many strategies have been proposed to preserve and at the same time remove moisture content of the paddy rice. For instance, Allaf et al. reported application of controlled pressure drop (DIC) process on post-harvest paddy rice. The DIC process included rapid heating of paddy rice at saturated pressure and then followed by abrupt reduction in pressure to roughly 4–5 kPa. Results showed that drying time of the paddy rice treated using DIC process was decreased six-folds compared with the untreated sample of paddy rice [6]. Pan et al. reported removal of moisture from medium grain rice through infrared radiation heating mechanism. A specific infrared power of 5,348 W/m^2 when applied was found decrease moisture content of rice samples by approximately 3.2 to 3.8 % at operation temperature of 63.5 ^{o}C [7]. The drying time of rice under infrared-assisted heating was only 58s, which was relatively small compared with hot air heating system [8].

For a natural drying process, heat and moisture transfer occurred mainly through force convection formed by rapid air flow inside the system. One of the main factors that affect air flow is porosity of the stored grain, which is related to the shape and size of the grain. A reduction in grain size was found to increase air flow resistance [9]. Currently, the main problem in storage facilities is the non-uniformity of air velocity which cause moisture and heat buildup inside the stored grain. Air velocity non-uniformity is the result of changes in porosity throughout the storage due to accumulation of small sized grain at the core of the facility and whole grain at the periphery [10]. Non-uniformity factor (NUF) can be calculated by equation 1 given the air velocity at the core and periphery of the storage room [11].

$$NUF = \frac{AF_p - AF_c}{AF_p + AF_c} \times 100 \tag{1}$$

Where AF_p is air flow velocity at the periphery air and AF_c is the core or centre air flow velocity.

Simulation of non-uniform air velocity in natural drying process have been observed in many researches. One of the first air flow resistance model was developed in 1980 using the Ergun's equation [12]. Finite volume method was also developed and solved using computational fluid dynamics (CFD) to find the non-uniform distribution of air velocity. It was revealed that the placement of ring duct at the bottom of the storage facility resulted in a more uniform airflow distribution [13]. Baffles can be added to the ventilation system to create a more uniform air flow [14]. A RANS k-ε model for simulation of turbulent system was found to be accurate compared with experimental validation results [15]. Shahid et al. analyzed the performance of a passive approach to dry and cool simple battery pack. Results demonstrated that addition of a secondary inlet pletnum on top of battery packs was found to be the most efficient method to improve air flow velocity and the cooling rate [16,17].

The aim of this research is to investigate simulation of three different model of room for storage of paddy rice. A CFD analysis was employed to calculate air flow velocity and temperature inside the storage facility. A two equations turbulence system was employed in this research. Model A represented a doom-like shaped roof, while Model B and Model C contained gable-like and pyramid-like shape roof.

2. Methods and Materials

2.1. Numerical algorithm and governing equation

The governing equations were solve using a CFD software FLUENT through fundamental finite volume approximation. The system domain for air flow was set as steady-state, incompressible with a 3-D turbulent type. The governing equations are derived from two main mechanisms in operation including continuity (equation 2) and momentum (equation 3) .

$$\frac{\partial \rho}{\partial t} + \frac{\partial (\rho u_i)}{\partial x_i} = 0 \tag{2}$$

$$\frac{\partial(\rho u_i)}{\partial t} + \frac{\partial(\rho u_i u_j)}{\partial x_i} = -\frac{\partial(P)}{\partial x_i} + \rho g_i + \frac{\partial\left[(\mu + \mu_t)\left(\frac{\partial u_i}{\partial x_j} + \frac{\partial u_j}{\partial x_i}\right)\right]}{\partial x_j} - S_i \quad (3)$$

$$P = p + \frac{2}{3}\rho k \quad (4)$$

$$S_i = -\left(D_{ij}\mu u + C_{ij}\frac{1}{2}\rho u^2\right) \quad (5)$$

Where ρ is the density (g/cm^3), t is time (s), u_i and u_j are the average superficial velocity components (m/s), k is the turbulent energy (m^2/s^2), g_i is gravity (m/s^2), μ is the viscosity of the medium (Pa s) and S_i is the source term equation or rate of strain tensor reflecting the normal viscous resistance (D_{ij}) and inertia resistance (C_{ij}) matrices for each material. A k-ε turbulent model (kinetic and turbulent dissipation) was used in the CFD analysis of air flow in the storage facility, as shown in equation 6 and 7. These 2 equation were employed to investigate the effect of turbulence on mean flow by solving the above governing equations entailing kinetic energy (k) and turbulent dissipation (ε) [18,19]. Other simulation have employed this turbulent model including agricultural engineering [20], air flow in greenhouses [17,21,22], and hydropower stations [14] .

$$\frac{\partial k}{\partial t} = \frac{\partial[\left(\mu + \frac{\mu_t}{\sigma_k}\right)\frac{\partial k}{\partial x_j}]}{\partial x_j} + \mu_t S^2 - \rho\varepsilon \quad (6)$$

$$\frac{\partial \varepsilon}{\partial t} = \frac{\partial[\left(\mu + \frac{\mu_t}{\sigma_\varepsilon}\right)\frac{\partial \varepsilon}{\partial x_j}]}{\partial x_j} + \frac{\varepsilon}{k}(C_{1\varepsilon}\mu_t S^2 - \rho\varepsilon C_{2\varepsilon}\varepsilon) \quad (7)$$

Where $C_{i\varepsilon}$, σ_k, and σ_ε are constants, S is the mean modulus, σ_k is a Prandtl number based turbulence constant and μ_t is the mean turbulent viscosity. These 2 equation turbulent technique were found to be better than standard method because it allow calculation and clear visualization of vortices

2.2. *Geometry and boundary conditions*

A three-dimensional type of rice paddy storage facility was employed for air flow and temperature simulation. The storage facilities are 3 meter wide, 8 meter long and 3 meter high. Three different model, drawn by ANSYS software, were used in the simulation as shown in Figure a, b and c. The roof use in this model was assumed to be a very excellent conduction of heat. Additionally, reflected heat radiation is indicated in the model as the hot layer at the bottom of the model. Air was assumed to enter from the left and right side of the storage facility.

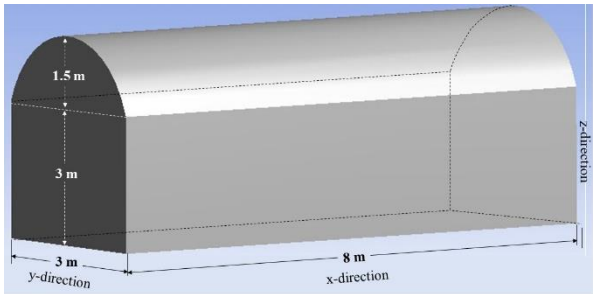

(a)

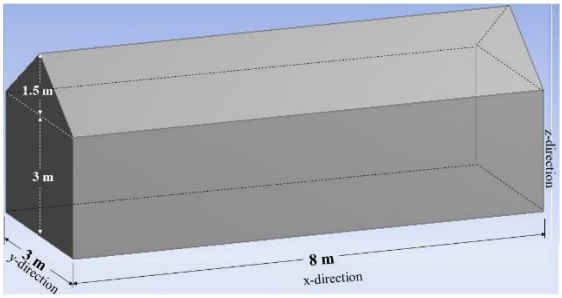

(b)

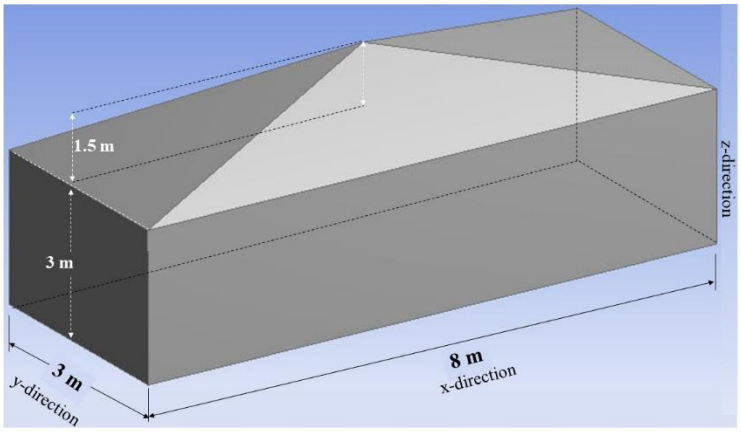

(c)

Figure 1. The geometry of the three different paddy rice storage facilities
a) doom-like Model A, b) gable-like Model B and c) pyramid-like Model C.

2.3 Boundary conditions

The boundary condition at the entrance was calculated by using air volume which was assumed to be a single component model, incompressible and steady-state flow medium. The air pressure at the inlet and outlet was set at 101,325 Pa as shown in Table. Simulation was conducted based on density and heat flux at the walls were set at 800 W/m^2.

Table 1 Boundary conditions for CFD analysis

Boundary condition	**Pattern**
Inlet boundary condition	Pressure inlet 101,325 Pa
Outlet boundary condition	Pressure outlet 101,325 Pa
Solver	Density Base Type implicit
Time	Steady state
Near-wall treatment method	Standard wall function
Turbulence model	The RNG k-ε model
Radiation model	Discrete Ordinates (DO)
	Type Full Buoyancy Effect
Heat flux	Wall Heat flux 800 W/m^2

3. Results and discussion

The outcomes of CFD simulation from three difference model of paddy rice storage facility are shown in below. Figure 2 demonstrated the speed vector at different location inside the room. The colour and length of the vector is associated with the magnitude of speed vector. Air flow in the doom-shape (model A) room was relatively less intense compared with airflow in the other two models. A vague vortex was formed at the right side of Model A. Figure 2a demonstrated that airflow inside model B seemed to change direction more than Model A. This indicated better ventilation and airflow that is more intense, which correspond well with another research [23]. Model C, as shown in Figure 2c, seemed to have

the most intense airflow with 7 small vortex and 2 larger vortex approximately 30 cm above the ground. These intense radial vortex airflow pattern created air curtain that effectively suppressed particle and increase ventilation inside the storage facility [24].

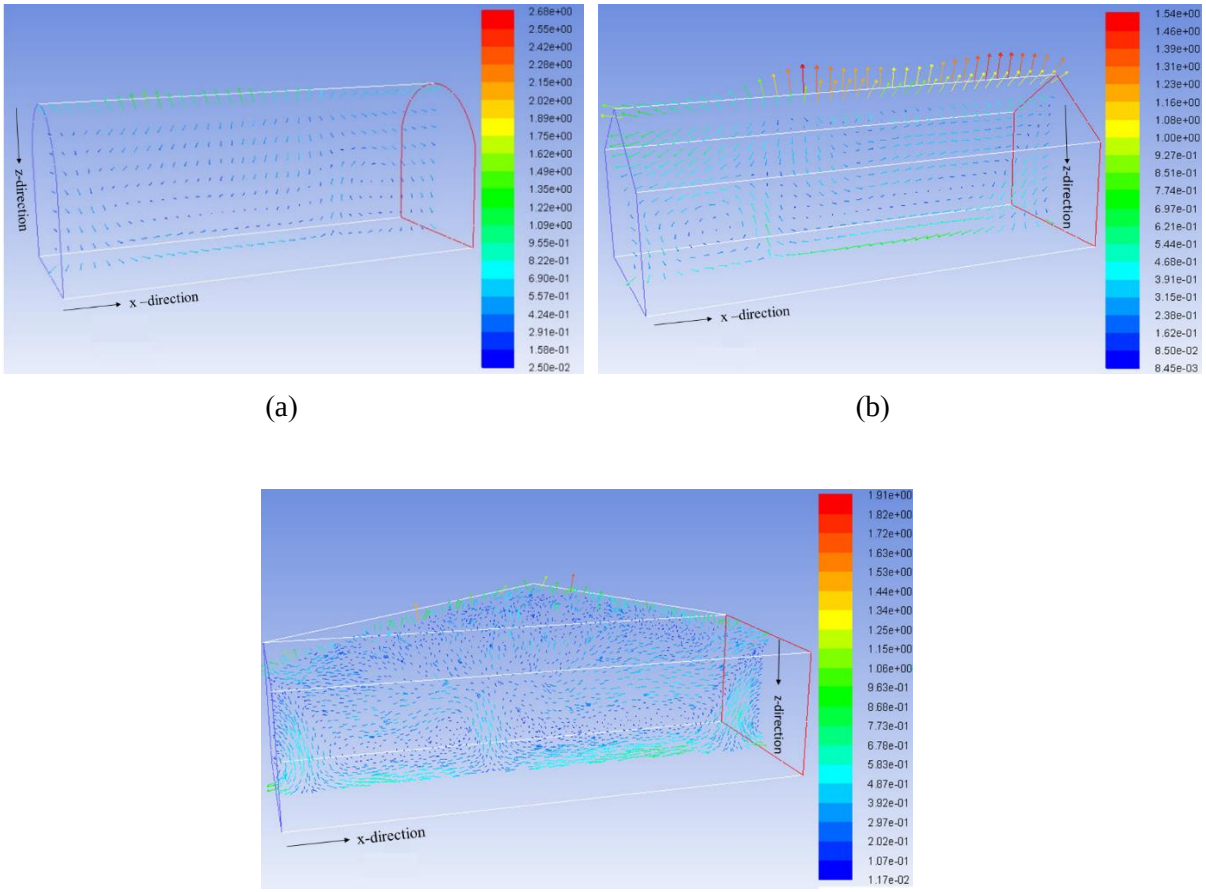

(a) (b)

(c)

Figure 2. Speed vector for a) Model A, b) Model B and c) Model C.

Figure 3 illustrated the speed velocity (m/s) at all location considering the cross-sectional area inside the storage facility. These contour plots were found to correspond with the speed vector shown in Figure 2. Simulation of Model A revealed large area of relatively slow airflow (0.16 – 0.21 m/s) in the centre of the storage facility. Additionally, airflow along the floor in Model A was relatively slow as well indicating ineffective ventilation. The slow airflow area diminished as Model A was changed to Model B. Rapid airflow (0.37 - 0.48 m/s) emerges at the top left of Model B and drop down toward the floor along the x-direction. A significant decrease in rapid airflow area was illustrated in Model C, which have a pyramid-like shaped roof. Figure 4 compared airflow along the x-direction and 30 cm above the storage room floor of three different models. Model C demonstrated lowest air speed at all the location along the x-direction. The average air speed inside Model A and Model B were similar at approximately 0.31 m/s, while Model C gave half the average air speed compared with the other models. However, the air distribution inside Model C storage facility is clearly more uniform.

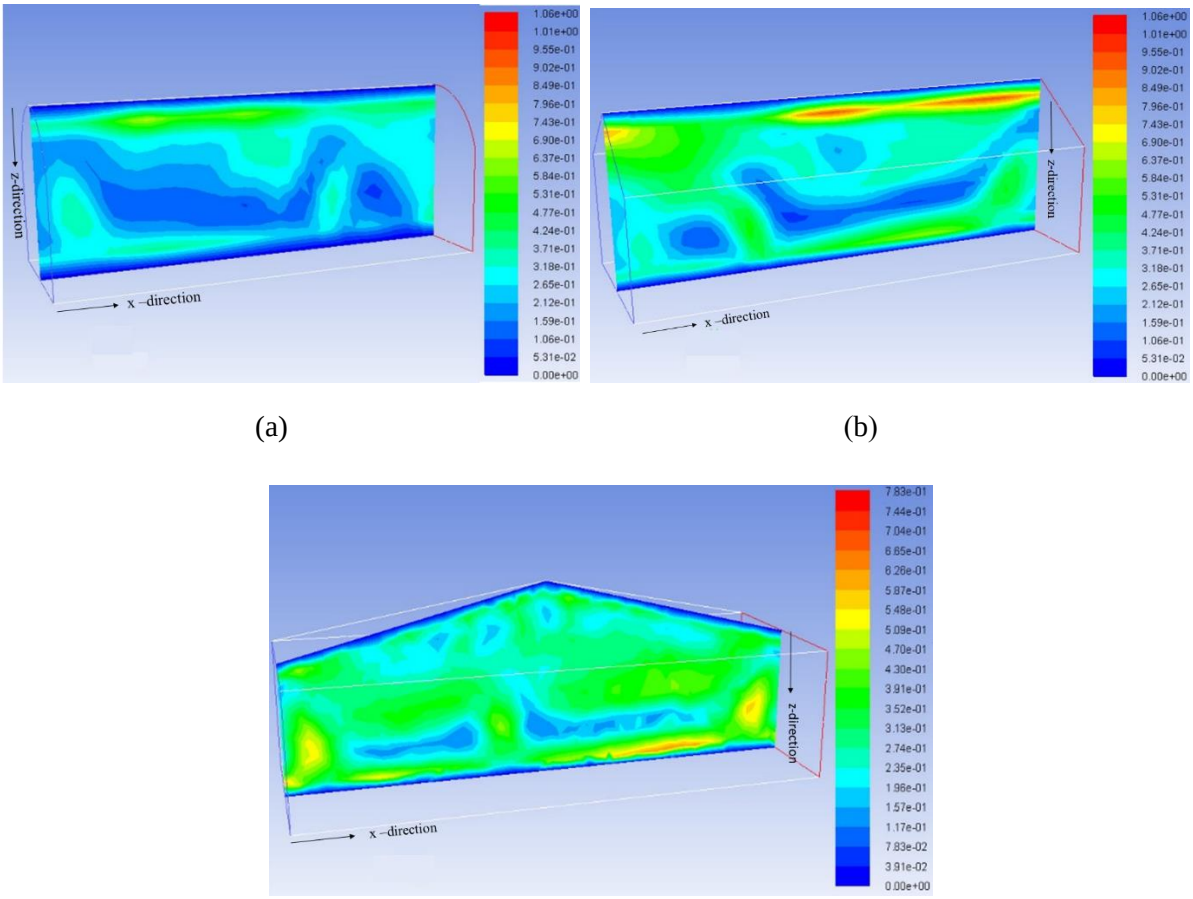

Figure 3. Cross sectional contour plot of air speed (m/s) inside a) Model A, b) Model B and c) Model C storage facility

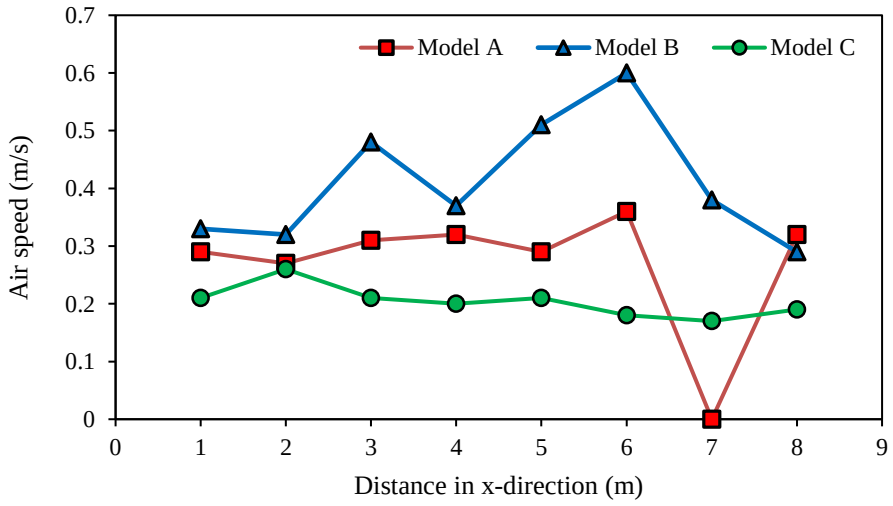

Figure 4. Air speed along the x-direction from the left-side of storage room and 30 cm above the floor.

Figure 5 demonstrated the air temperature profile of the three different models. In these models heat is transferred from the roof of the storage facility through convection and radiation. The temperature of the storage room's roof was 417 to 433 K which had been considered as an effective heat source for the simulation model. It was observed that the storage floor also emitted heat. The floor-leveled heat originated partially from reflected heat and also from radiation. For all models air temperature decreased gradually in form of uniform air temperature layer in the x-direction, which is the direction from the roof toward the floor as shown in Figure 5a - c. Simulated air temperature along the x-direction 30 cm above floor were shown in Figure 6. Model C was found to have higher air temperature at each location along the x-direction compared with the other models. This may be due to the low air velocity simulated in Model C. Lower air velocity area help maintain heat inside the storage room, while rapid air velocity initiate heat loss. The results corresponded well wither another research [25]. It can also be observed from Figure 6 that the temperature layer along the vertical x-axis from the roof changed more rapidly inside Model A and Model B compared with Model C. Air temperature and speed measurement have been conducted at different location inside the storage facility of Model A to validate the mathematical modelling concept use in the simulation. Validation revealed the collected data to be closed to simulated results with r-square close to 0.98.

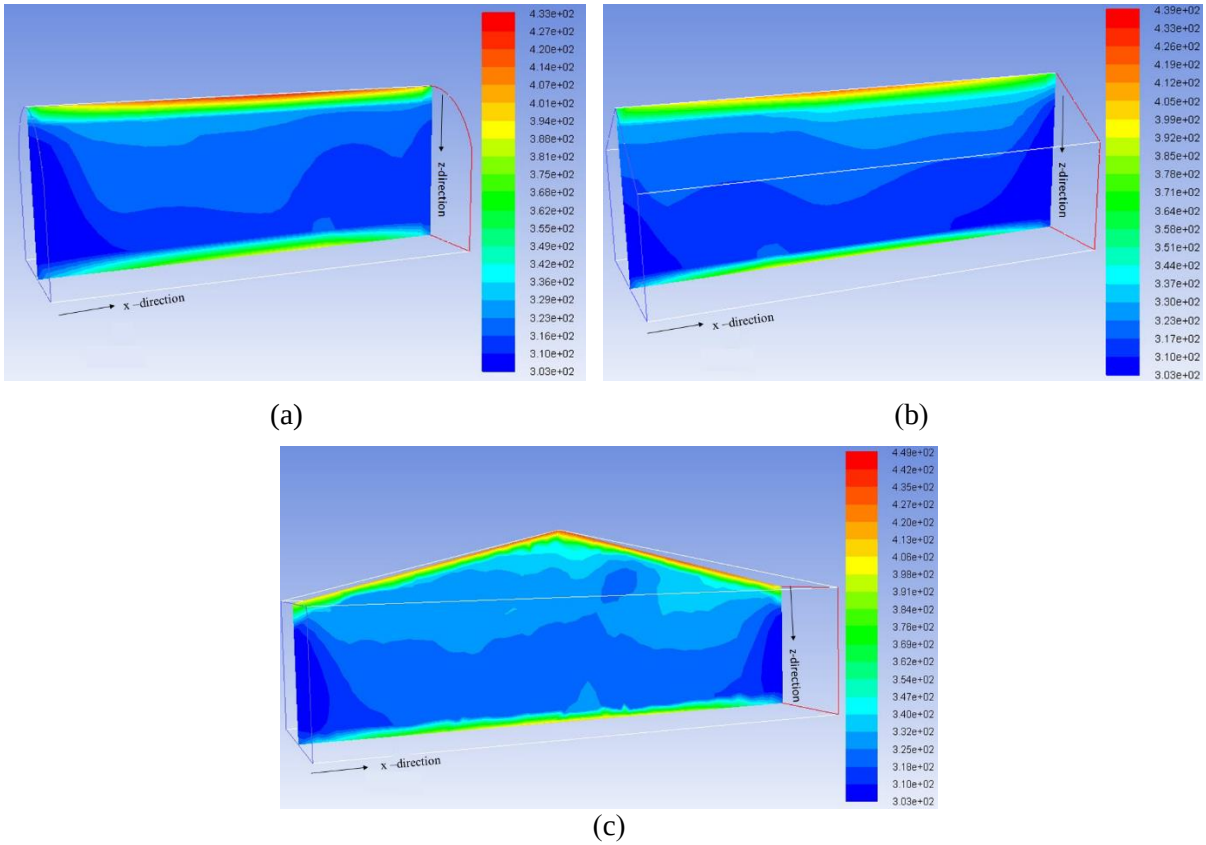

Figure 5. Cross sectional contour plot of air temperature inside a) Model A, b) Model B and c) Model C

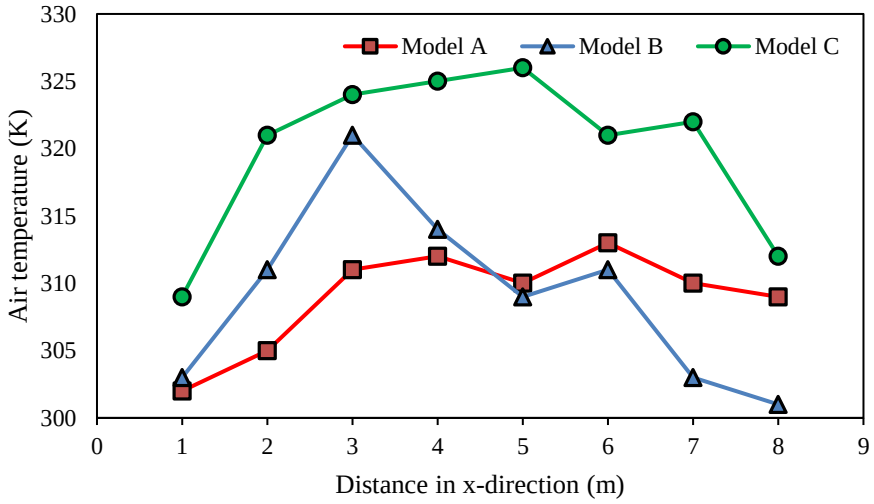

Figure 6. Air temperature along the x-direction from the left-side of storage room and 30 cm above the floor.

Conclusion

The effect of storage's roof geometry on the airflow pattern, speed and temperature were studied. Air speed vector demonstrated intense radial vortex inside Model C storage room with pyramid shape roof, indicating turbulent airflow behaviour. The air speed inside Model C was significantly lower than storage facility with dome and gable shape roof. However, airflow speed in Model C was found to be more uniform compared with the other two type of models. The low air speed in Model C resulted in an increase in convective heat transfer resistance which reduced heat loss and ultimately maintain higher air temperature compared with the average temperature inside storage facility with dome and gable shape roof. This research demonstrated the potential of a pyramid-like room to be used for storage and drying of rice paddy. Simulation using CFD analysis is an effective technique that can be employed to overcome time consuming and costly process that decision maker need to undergo in order to understand the effect of storage room facility.

Acknowledgments

The author would like to thank the Faculty of Engineering, Thammasat University for providing the necessary research funding for this project.

References

[1] Seck PA, Diagne A, Mohanty S, Wopereis MCS 2012 *Food Security* **4**(1) 7-24.
[2] Sumithra M, D SJ, Scott M, F MG 2014 *Annals of the New York Academy of Sci*. **1324**(1) 7-14.
[3] Normile D 2010 *Sci*. **321** 330-3.
[4] Sombunjitt S, Sriwongchai T, Kuleung C, Hongtrakul V 2017 *Agricul*. *Nat*. *Res*. **51**(5) 365-75.
[5] Bartosik R, Maier D 2006 *Transactions of the ASABE* **49**(4) 1095.
[6] Mounir S, Allaf K 2014 DIC-Assisted Hot Air Drying of Post-harvest Paddy Rice. In: Allaf T, Allaf K, editors. Instant Controlled Pressure Drop (DIC) in Food Processing: From Fundamental to Industrial Applications. New York, NY: Springer New York 45-55.
[7] Ragab K, Zhongli P, F TJ, S ESA, R HB, S EAM 2014 *J*. *Food Proc*. *and Preserv* **38**(1) 430-40.
[8] Ding C, Khir R, Pan Z, Wood DF, Venkitasamy C, Tu K 2018 *Food Chem*. **264** 149-56.
[9] S Chung D, Maghirang R, S Kim Y, S Kim M 2001 *Transactions of the ASAE* **44**(2) 331–336.
[10] Lawrence J, Maier DE 2011 *Biosys*. *Engin*. **110**(3) 321-9.
[11] Bartosik RE, Maier DE 2006 *Transactions of the ASABE*;49(4):1095-104.

[12] Lai FS 1980 *Transactions of the ASAE* **23**(3) 729.
[13] Garg D, E Maier D 2006 *9th International Working Conference on Stored Product Protection* 7-12.
[14] Ye W-B. 2017 *Appl. Ther. Engin.* **110** 573-83.
[15] Fuentes-Pérez JF, Silva AT, Tuhtan JA, García-Vega A, Carbonell-Baeza R, Musall M 2018 *Environ. Model. Soft.* **99** 156-69.
[16] Shahid S, Agelin-Chaab M 2018. *Ther. Sci. Engin. Prog.* **5** 351-63.
[17] Zhang Y, Kacira M, An L 2016 *Biosys. Engin.* **147** 193-205.
[18] Liu N, Wang W, Wang Y, Wang Z, Han J, Wu C 2017 *Appl. Ther. Engin.* **125** 1209-17.
[19] Jiru T, Bitsuamlak G. 2010 Int. J. Ventilation **9**(2) 131-47.
[20] Bustamante E, García-Diego F-J, Calvet S, Estellés F, Beltrán P, Hospitaler A 2013 Energies **6**(5) 2605.
[21] Bournet PE, Ould Khaoua SA, Boulard T 2007 *Biosys. Engin.* **98**(2) 224-34.
[22] Rohdin P, Moshfegh B. 2007 *Building and Environ.* **42**(11) 3872-82.
[23] Khatchatourian OA, Binelo MO. 2008 *Biosys. Engin.* **101**(2) 225-38.
[24] Nie W, Wei W, Cai P, Liu Z, Liu Q, Ma H 2018 *Advanced Powder Technol.* **29**(3) 835-47.
[25] Ferrua MJ, Singh RP. 2011 *Procedia Food Sci.* **1** 1239-46